

MICROSTRUCTURE MODIFICATION AND DEFORMATION BEHAVIOR OF FINE GRAINED AZ61L SHEET PRODUCED BY THIXOMOLDING® AND THERMOMECHANICAL PROCESSING

T.D. Berman¹, W. Donlon¹, V.M. Miller³, R. Decker², J. Huang², T.M. Pollock³, J.W. Jones¹

¹Materials Science and Engineering, University of Michigan, 2300 Hayward St; Ann Arbor, MI, 48109, USA

²nanoMAG, LLC., 13753 Otterson Court; Livonia, MI, 48150, USA

³Materials Department, University of California, Santa Barbara; Santa Barbara, CA, 93106-5050, USA

Keywords: AZ61L, Microstructures, Texture, Mechanical Properties, Thixomolding, Thermomechanical Processing

Abstract

X-ray diffraction and hardness measurements are used to study recrystallization in fine-grained AZ61L sheet produced by warm-rolling of Thixomolded® material. The as-rolled sheet is partially dynamically-recrystallized, with a strong basal texture and a sub-micron grain size. Significant increases in ductility with moderate reductions in tensile strength were produced by annealing at temperatures greater than 250 °C. A weakening in basal texture was observed in samples annealed at over 250 °C. Static recrystallization was determined to be responsible for the reduction in texture and associated increase in elongation.

Introduction

Lightweighting requires engineering high strength magnesium sheet with good formability; the limited formability is the most significant hindrance to the implementation of Mg-sheet. A strong basal texture exists in Mg-alloy sheet due to the preponderance of deformation by slip along the close-packed basal planes [1]. This basal sheet texture is unfavorable for through-thickness deformation. Weakly textured or non-textured sheet is desirable. In addition to texture modification, grain size refinement is also an essential mechanism to improve both the strength and ductility of Mg-alloys [2, 3].

The fine grain structure of Thixomolded Mg-alloys is advantageous for thermomechanical processing to finer grain sizes. Sheet produced by Thixomolding and Thermomechanical Processing (TTMP) has shown strength and ductility in excess of 300 MPa and 6% respectively [4]. Post-processing annealing of TTMP material has produced sheet with lower strength (~230 MPa) but ductilities near 20% [4]. The strong basal texture imparted by rolling has been alleviated in post-processing annealing [4].

Experimental

Preheated Thixomolded plates, with dimensions of 200 mm x 200 mm x 3 mm, were warm-rolled with a roll temperature near 200 °C to a thickness reduction of approximately 50%. Table 1 gives the composition of the AZ61L plates. Dogbone tensile specimens with a gauge length of 31.75 mm and cross section of 7.94 mm, were machined from the sheets with the tensile axes parallel to the rolling direction. Room temperature tensile tests were performed with a displacement rate of 0.71 mm/min. An extensometer was used to measure tensile elongation. Vickers hardness measurements were taken with a Clark Microhardness tester with a dwell time of 15 s and a 200 g load.

All microscopy and texture measurements examine the polished surface of the sheet. SEM and XRD samples were prepared by polishing to 1 μm diamond paste and then etching for 10 s at room temperature in a 1:9 solution of o-phosphoric acid in ethanol. TEM specimens were prepared by dimpling and ion milling using a Gatan Precision Ion Polishing System (PIPS). TEM was conducted with a Phillips CM12 AEM system. Electron Backscatter Diffraction (EBSD) specimens were prepared by polishing to 1 μm diamond paste followed by ion polishing in a Gatan PIPS. EBSD examination was conducted with a Philips XL30 FEG equipped with a TexSEM Laboratories OIM system. A step size of 0.25 μm was used for EBSD measurements. A Rigaku rotating anode XRD system was used to make XRD pole figure measurements.

Table 1: Composition of received AZ61L in wt %

Al	Zn	Mn	Si	Fe	Mg
6.5	0.46	0.14	0.01	0.003	bal.

Table 2: Tensile properties of annealed sheet

Sample	YS (MPa)	UTS (MPa)	El (%)
as-Rolled	311.2 ± 15.5	369.6 ± 13.3	8.3 ± 2.6
TTMP + 250 °C 3 min Anneal	331.5 ± 6.4	372.3 ± 5.4	5.5 ± 2.4
TTMP + 250 °C 10 min Anneal	313.0 ± 17.2	365.3 ± 8.0	5.6 ± 3.4
TTMP + 250 °C 20 min Anneal	321.7 ± 3.1	361.3 ± 2.3	7.2 ± 1.4
TTMP + 275 °C 15 min Anneal	231.7 ± 1.7	306.6 ± 4.4	13.8 ± 4.0
TTMP + 300 °C 3 min Anneal	236.7 ± 4.1	315.3 ± 1.3	15.5 ± 2.1
TTMP + 300 °C 5 min Anneal	266.2 ± 5.6	336.0 ± 4.4	14.1 ± 3.1
TTMP + 300 °C 10 min Anneal	223.6 ± 1.2	308.5 ± 4.8	16.6 ± 3.0
TTMP + 300 °C 20 min Anneal	216.5 ± 5.7	307.6 ± 1.4	22.5 ± 1.5
TTMP + 300 °C 30 min Anneal	203.7 ± 6.5	306.8 ± 1.8	19.7 ± 4.3

Results

Mechanical Properties

Vickers microhardness measurements (Figures 1 and 2) illustrate that softening occurs when annealing above 250 °C. The as-rolled sheet has a Vickers microhardness measurement of 98 ± 3 HV. Coupons subjected to thermal exposures at 130, 170, and 210 °C exhibit a small drop in hardness following five minutes of annealing. After a few hours at these low temperatures, the hardness stabilizes at approximately 94 HV.

A different behavior is seen at annealing temperatures above 250 °C. Ten minute annealing treatments reveal a precipitous decay between the maximum and minimum hardness. The drop in hardness after annealing for 5 minutes at 300 °C is significant, especially when compared to the lower temperature anneals. After annealing at 300 °C for 20 h, the longest annealing treatment considered in this study, the hardness has dropped 30 points to 68 ± 3 HV.

A similar temperature effect is seen in the strength measurements (Table 2). The tensile properties of the samples annealed at 250 °C for 3, 10, or 20 minutes show little change from the as-rolled condition. Samples subjected to annealing above this temperature lose about 90 MPa in yield strength. Elongation of the samples annealed above 250 °C doubles.

Microstructure

The Thixomolded microstructure consists of α -Mg grains with an average diameter of 4 μm surrounded by a divorced eutectic of β - $\text{Mg}_{17}\text{Al}_{12}$ (Figure 3). The β particles are heterogeneously distributed throughout the plate, with a volume fraction of approximately 3%. The as-molded material is untextured.

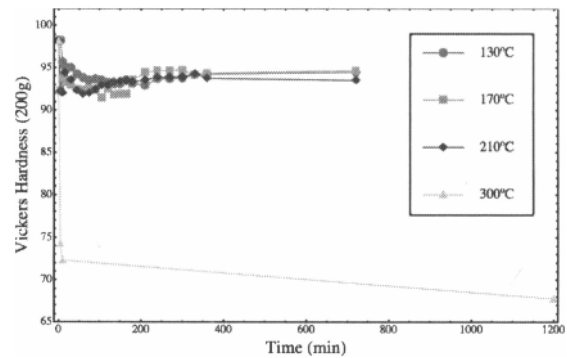


Figure 1: Isothermal microhardness measurements of annealed sheet. When going from 210 °C to 300 °C a significant difference in behavior is seen. To improve readability, error bars are not shown; the maximum error is ± 3.1 HV.

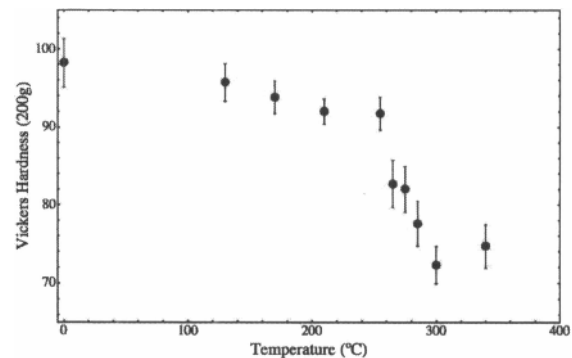


Figure 2: Microhardness measurements of sheet annealed for 10 minutes.

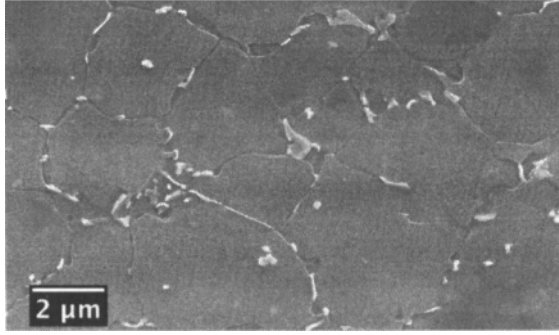


Figure 3: SEM image of Thixomolded AZ61L microstructure. The bright particles are the β phase.

Partial dynamic recrystallization occurs during the rolling process, as shown in the inverse pole figure map displayed in Figure 4. The fraction recrystallized, roughly estimated by the fraction of points indexed as Mg with a confidence index greater than 0.5%, is 17%. The recrystallized regions have a sub-micron grain size (Figure 5). The β particles in the as-rolled sample are smaller than those observed in the as-molded alloy. Coherent lath β precipitates are seen in some regions, these precipitates have a Burgers orientation relationship, $[1\bar{2}10]_{Mg} // [1\bar{1}1]_{\beta}$ (Figure 6). The overall spatial distribution of β particles remains largely unchanged from that seen in the as-molded condition.

Crystallographic Texture

The macroscopic as-rolled sheet texture, as measured by XRD, shows a double-peaked basal texture with a maximum intensity of 3 multiples of random distribution (MRD) (Figure 7). The distribution spread is wider along the transverse direction. This double peak is likely due increased activity of the non-basal $\langle c+a \rangle$ slip mode [5, 6].

XRD basal pole figures of annealed samples illustrate weakening of the basal texture at annealing temperatures above 250 °C. The texture remains unchanged after annealing at 210 °C for 12 hours. In contrast, a large change in texture can be seen after 5 minutes at 300 °C. Further weakening of the basal texture occurs after annealing for 35 minutes at 300 °C. The double-peak is no longer present in this annealing condition.

Discussion

The hardness and tensile measurements indicate that static recrystallization is occurring during the annealing process. The kinetics of the process seem to match well

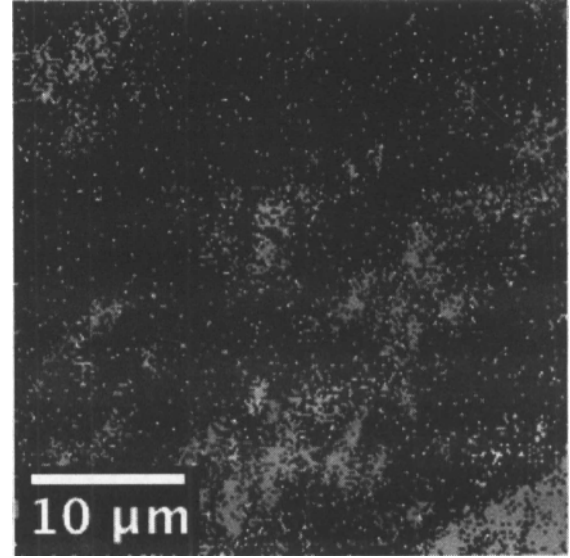


Figure 4: Inverse pole figure map of as-rolled sheet. Most of the sheet is not recrystallized, and thus not indexable by the EBSD technique.

with those of the Johnson-Mehl-Avrami-Kolmogorov (JMAK) theory. The fraction recrystallized can be approximated as the fraction softened [7, 8], defined as:

$$X = \frac{H_{AR} - H}{H_{AR} - H_{min}} \quad (1)$$

Here H_{AR} is the hardness of the as-rolled sheet and H_{min} is the hardness of completely recrystallized material. Here H_{min} is approximated as 72 HV, the average hardness of the four highest temperature annealing treatments. This data was then fit with the JMAK model expressed below [8, 9].

$$X = 1 - \exp(-0.693 (t/t_{0.5})^n) \quad (2)$$

where $t_{0.5}$ is the time to 50% recrystallization, which is calculated using Equation 3 [8].

$$t_{0.5} = BZ^r \exp(Q_{rex}/RT) \quad (3)$$

Z is the Zener-Holloman parameter:

$$Z = \dot{\epsilon} \exp(Q_d/RT_d) \quad (4)$$

R is the ideal gas constant (8.314 JK⁻¹mol⁻¹). The activation energy for self-diffusion, 135 kJmol⁻¹, is used to approximate, Q_d , the activation energy for deformation. T_d , the temperature of deformation, was approximately 300 °C. The expressions for $t_{0.5}$ and Z were substituted into Equation 2 and fit to our experimental

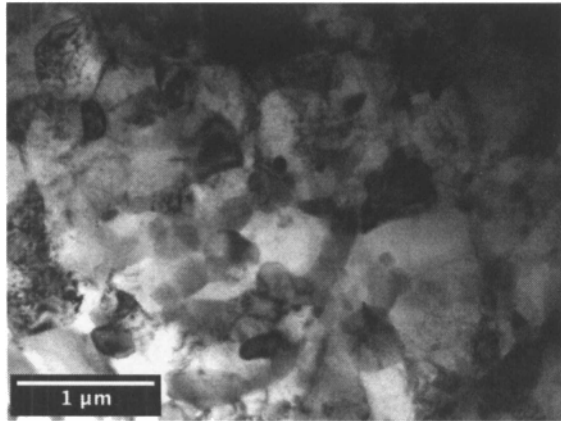


Figure 5: Microstructure of as-rolled sheet. This particular region exhibits a sub-micron dynamically recrystallized grain size.

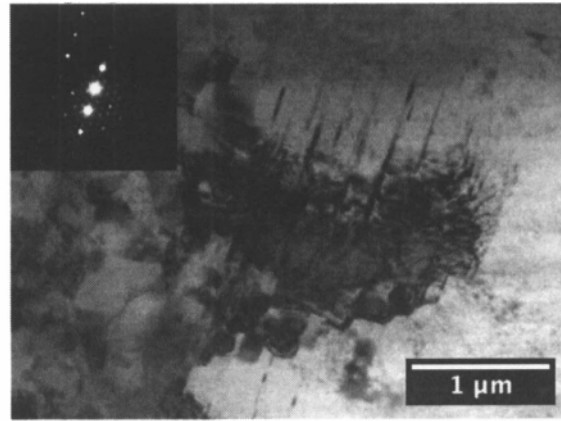


Figure 6: Coherent lath-shaped β precipitates in the as-rolled material. The selected area diffraction pattern indicates a Burgers orientation relationship.

Table 3: Parameters used for JMAK model

Parameter	Value
n	0.94
Q_{rex}	137 kJmol^{-1}
B	2.68
r	-0.87

data for the fraction recrystallized (Figure 8). A non-linear regression algorithm was used to solve for n (the Avrami exponent), Q_{rex} (the activation energy for recrystallization), and the fitting constants r and B. The best fit parameters are presented in Table 3.

An Avrami exponent of 0.94 is slightly lower than what has been calculated in deformed AZ-series alloys in other studies; reported Avrami exponents range between 1.18 and 1.38 [8, 10, 11]. As the Avrami exponent models the slope during the recrystallization process, more hardness measurements near 250°C could indicate that a steeper slope, and thus slightly higher value of n is more appropriate. Regardless, we observe an Avrami exponent are lower than the value of $n=4$ which is expected if the assumptions of the model for continuous nucleation and spherical growth are satisfied [12]. This low exponent may be due to non-random nucleation in the deformed material, for instance an exponent of 1 has been found when modeling nucleation of random sites on grain boundaries [13]. Clusters of β particles along grain boundaries may be preferential nucleation sites.

Particle stimulated nucleation (PSN) would also help to explain the texture weakening indicated in the XRD

pole figures. It is generally believed that static recrystallization does not appreciably alter the deformation texture [14, 15]. Limited twinning has been observed in this fine grained material, so that mechanism in texture reduction is unlikely. Dense clusters of β particles, produced in the warm-rolling process may be responsible for nucleating new, non-basal oriented grains. Future work will explore this further.

The reduction of basal texture leads to an improvement in the tensile elongation along the rolling direction. As annealing at 300°C progresses, and the basal texture weakens, the elongation increases (Table 2). After 3 minutes, at which point our model predicts the material is $\sim 60\%$ recrystallized, the elongation increases from 8% to 16%. At 20 minutes the elongation reaches 23%. No further improvement of elongation is seen by increasing the duration of annealing. This is expected if the improvement is indeed due to texture evolution during recrystallization, as our model predicts that recrystallization will be complete by 20 minutes at 300°C .

Conclusions

TTMP AZ61 sheet is only partially dynamically recrystallized, with a sub-micron grain size. Static recrystallization occurs during the annealing of the as-rolled sheet. A simple empirical model, based on JMAK theory, can be used to describe the recrystallization process. A low Avrami exponent of 0.94 was fit using this model, indicating non-random nucleation. XRD pole figure measurements reveal a weakening of the as-rolled near-basal texture during the static recrystalliza-

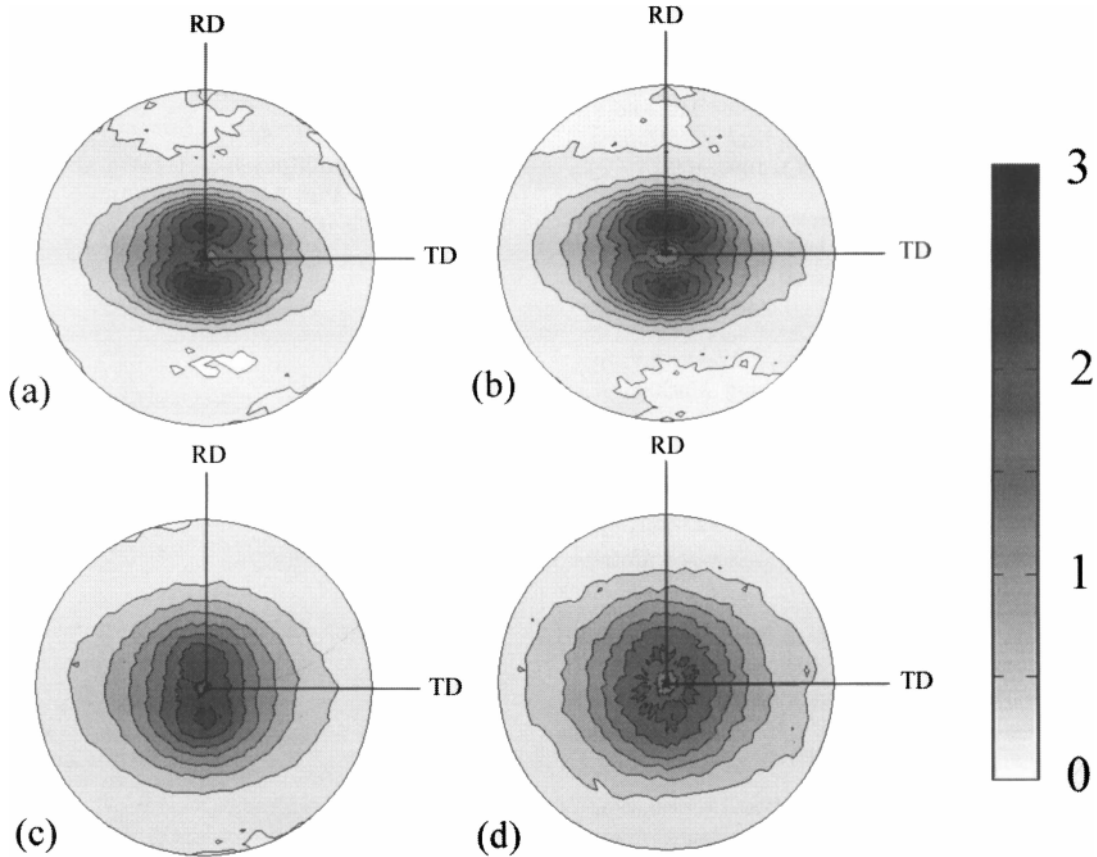


Figure 7: XRD (0002) pole figures of (a) as-rolled sheet, (b) sheet annealed for 12 hours at 210 °C, (c) sheet annealed for 5 minutes at 300 °C and (d) sheet annealed for 20 hours at 300 °C.

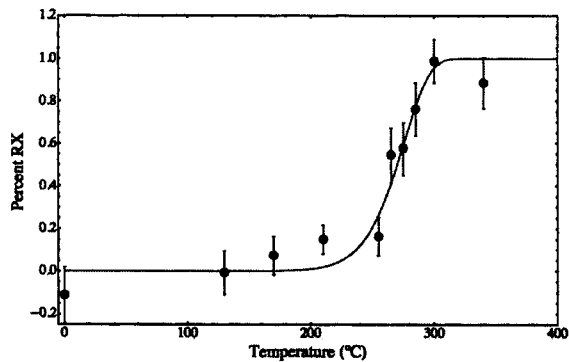


Figure 8: JMAK model for fraction recrystallized fit to fraction softening data. Isochronal curve for 10 minute anneal.

tion process. Ductility in the sheet improves as the texture is weakened. An understanding for the mechanism behind this texture randomization is needed to allow for better forming of Mg-alloy sheet.

Acknowledgements

This material is based upon work supported by the National Science Foundation under Grant No. 0847198. Many thanks to Garret Huff and Eric Hung for their assistance on this project.

References

1. Y. Wang and J. Huang, "Texture Analysis in Hexagonal Materials," *Materials Chemistry and Physics*, 81 (1) (2003), 11-26.
2. M. Barnett, D. L. Atwell, and A. Beer, "Grain Size in Mg Alloys : Recrystallization and Mechanical

- Consequences,” *Materials Science Forum*, 558-559 (2007), 433-440.
3. J. Koike, “Enhanced Deformation Mechanisms by Anisotropic Plasticity in Polycrystalline Mg Alloys at Room Temperature,” *Metallurgical and Materials Transactions A*, 36 (7) (2005), 1689-1696.
 4. T. D. Berman et al., “Microstructure Evolution in AZ61L During TTMP and Subsequent Annealing Treatments,” *Magnesium Technology*, eds. W. Sillekens et al. (Wiley, 2011), 599 - 603.
 5. S. Agnew, M. Yoo, and C. Tome, “Application of Texture Simulation to Understanding Mechanical Behavior of Mg and Solid Solution Alloys Containing Li or Y,” *Acta Materialia*, 49 (20) (2001), 4277-4289.
 6. A. Styczynski et al., “Cold Rolling Textures in AZ31 Wrought Magnesium Alloy,” *Scripta Materialia*, 50 (7) (2004), 943-947.
 7. A. Yanagida and J. Yanagimoto, “Formularization of Softening Fractions and Related Kinetics for Static Recrystallization Using Inverse Analysis of Double Compression Test,” *Materials Science and Engineering: A*, 487 (1-2) (2008), 510-517.
 8. A. Beer and M. Barnett, “The Post-Deformation Recrystallization Behaviour of Magnesium Alloy Mg 3Al 1Zn,” *Scripta Materialia*, 61 (12) (2009), 1097-1100.
 9. J. Li et al., “The Effect of Prestrain and Subsequent Annealing on the Mechanical Behavior of AA5182-O,” *Materials Science and Engineering: A*, 528 (10-11) (2011), 3905-3914.
 10. A. Beer and M. Barnett, “Microstructure Evolution in Hot Worked and Annealed Magnesium Alloy AZ31,” *Materials Science and Engineering A*, 485 (2008), 318-324.
 11. H. Chao et al., “Static Recrystallization Kinetics of a Heavily Cold Drawn AZ31 Magnesium Alloy Under Annealing Treatment,” *Materials Characterization*, 62 (3) (2011), 312-320.
 12. M. C. Weinberg, D. P. Birnie III, and V. Shneidman, “Crystallization Kinetics and the JMAK Equation,” *Journal of Non-Crystalline Solids*, 219 (1997), 89-99.
 13. J. Cahn, “The Kinetics of Grain Boundary Nucleated Reactions,” *Acta Metallurgica*, 4 (12) (1956), 449-459.
 14. X. Yang, H. Miura, and T. Sakai, “Recrystallization Behaviour of Fine-Grained Magnesium Alloy After Hot Deformation,” *Transactions of Nonferrous Metals Society of China*, 31 (2007), 1139-1142.
 15. R. K. Nadella, I. Samajdar, and G. Gottstein, “Static Recrystallisation and Textural Changes in Warm Rolled Pure Magnesium,” *Magnesium: Proceedings of the 6th International Conference Magnesium Alloys and Their Applications* (2005), 1052-1057.